

Effect of the synthesis conditions of titanium-magnesium catalysts on the composition, structure and performance in propylene polymerization

Natalya N. Chumachenko*, Vladimir A. Zakharov, Sergey A. Sergeev, Svetlana V. Cherepanova
Boreskov Institute of Catalysis, Siberian Branch, Russian Academy of Sciences,
Prospect Akademika Lavrentieva 5, Novosibirsk 630090, Russian Federation

Received: 20 July 2016, Accepted: 9 October 2016

ABSTRACT

Supported catalysts synthesized via the interaction of $\text{Mg}(\text{OEt})_2$ with TiCl_4 in the presence or absence of an internal stereoregulating donor (di-*n*-butyl phthalate), with different solvents (chlorobenzene, *n*-undecane, *n*-heptane) at different titanation temperatures have been studied by a set of physicochemical methods. Data on the chemical composition, X-ray structure and pore structure of these catalysts as well as data on their activity and stereospecificity in polymerization of propylene were obtained. Chemical composition, structure, activity and stereospecificity depend primarily on the presence of an electron donor stereoregulating component and on the solvent nature and titanation temperature. Activity of the catalysts is determined by totality of different characteristics: the chemical composition, in particular, the presence of inactive by-products like $\text{TiCl}_3(\text{OEt})$, the MgCl_2 X-ray structure and pore structure. More active catalyst which was synthesized under optimal conditions in the presence of di-*n*-butyl phthalate contains the minimal amount of $\text{TiCl}_3(\text{OEt})$ by-product, and has a more ordered X-ray structure and a homogeneous mesoporous structure with a narrow mesopore size distribution.

Keywords: Supported Ziegler-Natta catalysts; titanium-magnesium catalysts formation; propylene polymerization

INTRODUCTION

Modern processes of polypropylene (PP) production employ supported titanium-magnesium catalysts (TMCs) of the composition $\text{TiCl}_4/\text{D}_1/\text{MgCl}_2$, which consist of MgCl_2 as the support with TiCl_4 (the active component) and an electron donor compound (D_1 is the stereoregulating component) adsorbed on the support surface. TMCs can be synthesized by various methods, which differ mostly in composition of the initial magnesium compound that is used to obtain MgCl_2 with the required characteristics. Magnesium diethoxide is one of the most efficient precursors for TMC synthesis. Methods of TMC synthesis involving magnesium diethoxide, chemical and phase composition of TMCs, their pore structure, morphology and catalytic performance in propylene polymerization over such catalysts were reported in many works [1-18].

Additional treatments in an excess of titanium tetrachloride of the intermediate solid products obtained upon synthesis of such catalysts in the presence of benzoyl chloride were shown to exert a substantial effect on the catalyst composition, specific surface area, activity and stereospecificity in

* Corresponding Author-E-mail: chumach@catalysis.ru

polymerization of propylene [3, 8]. A catalyst synthesized using a mixture of internal donors (ethyl benzoate and diisobutyl phthalate) was studied in [17]. The size of MgCl_2 primary crystallites and activity of the catalysts were found to increase with raising the content of diisobutyl phthalate in a mixture of donors.

The catalyst formation by reacting magnesium diethoxide with titanium tetrachloride in the presence of di-*n*-butyl phthalate (DBP) as a stereoregulating electron donor was studied by characterization of the intermediate products during catalyst synthesis in [18]. Chemical and phase composition, pore structure, activity and stereospecificity of these products were investigated. It was shown that before addition of DBP, the X-ray amorphous product consisting of MgCl_2 and $\text{TiCl}_3(\text{OEt})$ was formed. This product had the micro-mesoporous structure, a very high surface area, but low activity and stereospecificity. DBP had a significant effect on both the chemical composition of the catalyst due to removing inactive $\text{TiCl}_3(\text{OEt})$, entering DBP and TiCl_4 in a solid product, and formation of MgCl_2 crystallites with the mesoporous structure. At the same time, a significant increase in the activity and stereospecificity was observed. A subsequent TiCl_4 /chlorobenzene treatment of the solid product completed these processes, provided some increase in the surface area at a similar mesoporous structure, and additionally increased activity and stereospecificity.

In the formation of this catalyst, of particular interest is the effect of internal donor on the catalyst composition, its crystal and pore structure. Besides, the literature provides insufficient data concerning the effect of solvents used in the catalyst synthesis and temperature of the synthesis on the composition, structural characteristics and performance of TMCs in polymerization of propylene.

In this work, titanium-magnesium catalysts were synthesized with magnesium diethoxide as a precursor upon variation of synthesis conditions: the presence or absence of internal donor (dibutyl phthalate), the use of a chlorinated aromatic solvent (chlorobenzene) or aliphatic solvents (heptane and undecane), and different temperatures of catalyst synthesis. The chemical and phase composition, pore structure and catalytic performance of these catalysts in propylene polymerization were studied to find correlations between catalytic performance and physicochemical characteristics of the catalysts.

EXPERIMENTAL

Materials

Reactive isopentane (*i*- C_5), *n*-heptane (*n*- C_7), *n*-undecane (*n*- C_{11}), chlorobenzene (ChB) and di-*n*-butyl phthalate (DBP) were preliminarily kept over molecular sieves and held in an argon atmosphere. TiCl_4 and $\text{Mg}(\text{OEt})_2$ (Aldrich) were used without additional purification.

Catalyst synthesis

The TMC-1catalyst has been prepared according to [18]. In this case the synthesis was performed via the interaction of $\text{Mg}(\text{OEt})_2$ with TiCl_4 in a chlorobenzene solution at a volume ratio $\text{TiCl}_4:\text{ChB} = 1:1$ and molar ratio $\text{DBP}/\text{Mg} = 0.15$ in four consecutive steps. At step I, a TiCl_4 solution in ChB and $\text{Mg}(\text{OEt})_2$ (molar ratio $\text{TiCl}_4/\text{Mg} = 13$) were introduced at room temperature in an argon atmosphere into a reactor

equipped with mechanical stirrer and placed in a thermostatically controlled bath. After that, the reactor temperature was raised from room temperature to 110°C at a rate of 1.5-2°C/min for 60 min. After reaching a temperature of 110°C, a sample of the suspension was transferred from the reactor to a vessel with heptane (60°C) (step I). Then DBP (DBP/Mg = 0.15) was introduced in to the reactor at 110°C. The reaction mixture was stirred at 110°C for 60 min. This was followed by the second sampling of the suspension (step II), sedimentation of the solid product, and decantation of the mother liquor. At step III, a TiCl₄/ChB solution (TiCl₄/Mg = 13, TiCl₄: ChB = 1:1 vol.) was added into the reactor with the solid product and held at 110°C for 60 min; this was followed by the third sampling of the reaction mixture. After decantation of the solution, step IV of the synthesis was carried out under conditions similar to those of step III, but the reaction mixture was held for 30 min. The TMC synthesis was completed by a repeated washing of the solid product with heptane; the washing temperature was gradually decreased from 70°C to room temperature. The samples taken during the synthesis were washed in a similar way. Prior to physicochemical studies, solid products were additionally washed with *i*-C₅. The samples were dried by evacuation at room temperature for 60 min and then at 50°C for 60 min.

The same technique was employed to synthesize catalysts TMC-2-TMC-5. The TMC-2 catalyst was obtained by the same procedure as TMC-1, but without DBP. The TMC-3 catalyst was synthesized similarly to TMC-1, but chlorobenzene was replaced with *n*-undecane. The TMC-4 catalyst was synthesized as TMC-1, but at 90°C instead of 110°C. The synthesis of TMC-5 was similar to that of TMC-1, but *n*-heptane was used instead of chlorobenzene and the synthesis was performed at 90°C instead of 110°C. General data on variation of the catalyst synthesis conditions are listed in Table 1.

Chemical analysis

The Ti and Mg content was found using inductively coupled plasma atomic emission spectroscopy (ICP-AES) on an Optima 4300DV (Perkin-Elmer) ICP spectrometer, and the Cl content was measured by potentiometric titration with an AgNO₃ solution after a preliminary dissolution of the catalyst in a 5% solution of sulfuric acid. The content of ethoxy groups was estimated by gas chromatography (NetChrom v2.0 software) with respect to ethanol after a preliminary dissolution of the sample in methyl cellosolve containing decyl alcohol as the internal standard. The content of dialkyl phthalates (DBP, ethylbutyl phthalate (EBP), diethyl phthalate (DEP) and phthaloyl dichloride (PC, (1, 2-benzenedicarbonyl dichloride)) was analyzed using liquid chromatography. The measurements were made on an LC-20 Prominence (Shimadzu) liquid chromatograph after a preliminary extraction of dialkyl phthalates and phthaloyl chloride from the solid product by acetonitrile.

Pore structure

Pore structure of the samples was analyzed by low-temperature nitrogen adsorption on an ASAP 2400 Micromeritics instrument. The adsorption measurement data were used to calculate specific surface area

(S_{BET} , m^2/g) and total pore volume (V_{total} , cm^3/g), which was estimated from the maximum adsorption obtained in the study.

Pore volumes and pore size distributions were calculated by BJH method using the adsorption branch of the isotherm. Results of calculation are presented in two modes. The first approach, as distribution cumulative pore volume versus average pore diameter (D) for the pore size range 2-100 nm. The second approach, as percentage of incremental pore volume (V_i) of the maximum incremental pore volume (V_i^{max}) versus average pore diameter. The latter method allows comparison of porosity of catalysts which differs sharply on the total pore volume.

XRD analysis

XRD patterns of the final catalysts were recorded on an X-ray diffractometer D8 ($\text{Cu}_{K\alpha}$ radiation, one-dimensional multichannel detector LynxEye) in the range of $5\text{-}90^\circ$ 2θ by scanning with a step of 0.05° and accumulation time of 2 s. Previously the samples were placed into a closed sample holder under argon in a glove box.

Interplanar distances were calculated using the Bragg equation from the 003 peak position. Average crystallite sizes (ACS) in the two perpendicular directions [001] (normal to the layers) and [110] (along the layers) were calculated using the Scherrer equation from the widths of (003) and (110) peaks, respectively.

XRD patterns for turbostratically disordered (TD) MgCl_2 were simulated by a program [19, 20]. The calculations were based on the model of a one-dimensionally (1D) disordered crystal. The model represents a sequence of Cl-Mg-Cl layers that can be shifted relative to each other by random vectors distributed by the Gauss law. XRD patterns of turbostratically disordered $\alpha\text{-MgCl}_2$ were simulated using absolute values of vectors (expressed in fractions of a cell size) of the mean square deviations (from 0 to 0.5) from equilibrium position. The turbostratic disorder degree (TDD) was obtained by multiplication of this value by two. A deviation of 0.5 gives a complete disorder and corresponds to a TDD equal to unity.

XRD patterns were simulated for the $\alpha\text{-MgCl}_2$ having different degrees of turbostratic disorder and average crystallite sizes of 6 nm. An increase in TDD introduced as the increase in mean square deviations of layers from their positions in $\alpha\text{-MgCl}_2$ leads to the broadening of all reflections except 00L and HK0. When mean square deviations reach half of the lattice parameter, TDD becomes full (equal to 1) and XRD patterns are represented by a reduced set of peaks, namely, 003 and 006 combined with the broadened 104, 110, 0012 and 0015 ones.

Polymerization of propylene

Polymerization of propylene was carried out in a 1 L steel reactor in a heptane medium. Before the reaction, a catalyst (10-12 mg) in a sealed ampoule was placed in a reactor, which was evacuated at 80°C for 1.5 h. After cooling the reactor to 25°C , heptane (300 ml), triethylaluminum cocatalyst ($[\text{AlEt}_3] = 4$ mmol/L), and propyltrimethoxysilane ($\text{PrSi}(\text{OMe})_3$) as an electron donor additive were introduced

successively at a molar ratio $\text{Al/PrSi(OMe)}_3 = 20$. After that, the ampoule with the catalyst was broken and the reaction mixture was held under stirring for 20 s. Hydrogen and propylene were then added into the reactor up to 0.5 atm. Prepolymerization was performed under the indicated conditions for 2 min. After that, the temperature and propylene pressure were raised to 70°C and 6 atm, respectively. Polymerization was carried out for 1 h at 70°C, a propylene pressure of 6 atm and a constant hydrogen/propylene molar ratio ($\text{H}_2/\text{C}_3\text{H}_6 = 0.013$).

Stereospecificity of the catalyst was estimated from the content of atactic PP (APP), which was found as the fraction of polymer dissolved in polymerization heptane.

RESULTS AND DISCUSSION

Chemical composition of catalysts

Table 2 lists data on the content of titanium, magnesium, chlorine, OEt groups and DBP for the catalysts obtained upon variation of the synthesis conditions (solvent, temperature, and presence or absence of DBP). Data on the content of Ti, Mg, Cl, OEt groups and DBP were used to calculate the composition of catalysts under the assumption that i) Mg(OEt)_2 completely converts to MgCl_2 ; ii) OEt groups enter the composition of ethoxytitanium chloride - $\text{TiCl}_3(\text{OEt})$; iii) a part of titanium is in the form of TiCl_4 since in all cases the OEt/Ti ratio is less than 1.

Effect of internal donor (DBP)

The key property of the internal donor (DBP) introduced in the TMC composition is its ability to enhance stereospecificity of the catalyst (isotacticity of the resulting PP). Therewith, DBP, which is introduced upon Mg(OEt)_2 interaction with TiCl_4 to obtain the MgCl_2 support, can exert a substantial effect on the chemical composition of the catalyst, its crystal and pore structure. Comparative data acquired in our study on the chemical composition of catalysts synthesized in the presence of DBP (TMC-1) and in its absence (TMC-2) are listed in Table 2. The TMC-2 catalyst (Table 2, exp. 2), which was synthesized without DBP, contains a much greater amount of titanium and OEt groups (8.5 and 4.2 wt.%) as compared to TMC-1 (exp. 1) (3.3 and 0.5 wt.%). The molar ratio $\text{OEt/Ti} = 0.53$ in the TMC-2 catalyst indicates that approximately a half of titanium compounds is represented by $\text{TiCl}_3(\text{OEt})$ in this case. Thus, in the absence of donor, $\text{TiCl}_3(\text{OEt})$ is strongly retained in the catalyst. As seen from data on the chemical composition (Figure 1a, b), in the case of TMC-2 catalyst, additional treatments of the solid product at steps III and IV in a TiCl_4/ChB medium are low efficient for removal of $\text{TiCl}_3(\text{OEt})$ formed at the first step of catalyst synthesis. In TMC-2, a part of titanium is present also as TiCl_4 because molar ratio OEt/Ti is equal to 0.53. By this means, according to the chemical analysis data, the TMC-2 catalyst has the composition $\text{MgCl}_2 \cdot 0.136 \text{ TiCl}_3(\text{OEt}) \cdot 0.122 \text{ TiCl}_4$. It is seen in the TMC-2 catalyst, titanium-containing compounds are present in two states: as TiCl_4 adsorbed on the MgCl_2 surface and as $\text{TiCl}_3(\text{OEt})$ or the $\text{TiCl}_3(\text{OEt})$ complex with MgCl_2 , which are the intermediate products in the synthesis of TMC-1. The

introduction of DBP after raising the temperature to 110°C results to efficient removal of the $\text{TiCl}_3(\text{OEt})$ by-product, and formation of the catalyst containing TiCl_4 adsorbed on MgCl_2 (catalyst TMC-1).

Effect of a solvent

The TMC-3 catalyst (Table 2, exp. 3), which was synthesized similar to TMC-1 (exp. 1) but with *n*-undecane instead of chlorobenzene, has a close to TMC-1 content of Ti, Mg and DBP. During the TMC-3 synthesis, the content of Ti and OEt groups in the solid product decreases, as in the case of TMC-1 (Figure 1a, b). Note that, in addition to DBP, the both catalysts contain EBP and DEP, which are formed in situ during the synthesis as by-products via the exchange of butoxy groups of DBP and ethoxy groups of $\text{Mg}(\text{OEt})_2$ or $\text{TiCl}_3(\text{OEt})$ [7, 9]. The TMC-3 catalyst has a higher content of OEt groups and the higher molar ratio $\text{OEt}/\text{Ti} = 0.29$ and accordingly $\text{TiCl}_3(\text{OEt})$ content. Solubility of $\text{TiCl}_3(\text{OEt})$ in a $\text{TiCl}_4/\text{C}_{11}$ medium may be lower in comparison with that in TiCl_4/ChB , thus increasing the fraction of titanium represented by $\text{TiCl}_3(\text{OEt})$ in the catalyst. In addition, TMC-3 has a high content of phthaloyl dichloride (5 wt. %), which forms by a side process of DBP chlorination with titanium tetrachloride [21]. According to the chemical analysis data, the composition of TMC-1 can be presented as $\text{MgCl}_2 \cdot 0.083 \text{TiCl}_4 \cdot 0.006 \text{TiCl}_3(\text{OEt}) \cdot 0.053 \text{DBP}$, and the composition of TMC-3 as $\text{MgCl}_2 \cdot 0.064 \text{TiCl}_4 \cdot 0.026 \text{TiCl}_3(\text{OEt}) \cdot 0.053 \text{DBP} \cdot 0.027 \text{PC}$. Thus, chlorobenzene as a component of TMC synthesis is more preferable than *n*-undecane, because the TiCl_4/ChB medium provides a more efficient removal of $\text{TiCl}_3(\text{OEt})$ and prevents the formation of phthaloyl dichloride (PC).

Effect of temperature

The synthesis of TMC at 90°C in a chlorobenzene medium in the presence of DBP produces the TMC-4 catalyst with the chemical composition close to that of TMC-1, which was obtained in the same medium but at 110°C (Table 2, compare exp. 4 and exp.1). These catalysts have a close content of titanium and a low content of ethoxy groups. Thus, a decrease in the synthesis temperature to 90°C with chlorobenzene as a solvent and in the presence of DBP does not produce a noticeable effect on the chemical composition of TMC.

The synthesis of TMC-5 at 90°C in a *n*-heptane medium gives quite a different composition of the catalyst in comparison with TMC-1 and TMC-4. The synthesis conditions of TMC-5 lead to the formation of the catalyst with a higher content of titanium, OEt groups and DBP (Table 2, exp. 5). As seen on Figure 1a,b, the content of titanium and ethoxy groups in solid products of TMC-5 remains virtually constant during the synthesis in the TiCl_4/C_7 medium. Despite the presence of DBP in the synthesis of TMC-5, a complete removal of OEt groups from its composition does not occur. A comparison of OEt/Ti molar ratios showed that in TMC-5 ($\text{OEt}/\text{Ti} = 0.44$) the content of titanium in the form of $\text{TiCl}_3(\text{OEt})$ was much higher than that in TMC-4 ($\text{OEt}/\text{Ti} = 0.16$). In addition, the TMC-5 catalyst contains a much greater amount of DBP (19 wt. %) as compared to TMC-4 (9.4 wt. %). The crystal structure of molecular complex $\text{TiCl}_4 \cdot \text{DEP}$ (DEP-diethyl phthalate), which was synthesized under the conditions close to those of TMC-5 catalyst (in a *n*-hexane medium), was characterized in [22]. Taking

into account these data, the high content of DBP and titanium can be attributed to the presence of solid complexes of titanium-containing compounds with DBP: $\text{TiCl}_3(\text{OEt}) \cdot m \text{DBP}$ and/or $\text{TiCl}_4 \cdot n \text{DBP}$, in the composition of TMC-5. In this case, the chemical analysis data listed in Table 2 imply that the $\text{TiCl}_4/\text{C}_7/\text{DBP}$ medium facilitates the formation of the TMC-5 catalyst with inhomogeneous composition, which comprises MgCl_2 with titanium tetrachloride adsorbed on its surface and the solid complex $\text{TiCl}_3(\text{OEt}) \cdot m \text{DBP}$ and/or $\text{TiCl}_4 \cdot n \text{DBP}$, which is insoluble in heptane at 90°C . The composition of TMC-4 can be presented as $\text{MgCl}_2 \cdot 0.135\text{TiCl}_4 \cdot 0.108\text{TiCl}_3(\text{OEt}) \cdot 0.12 \text{DBP}$.

A different pattern is observed in the case of TMC-3 (Table 2, exp. 3) and TMC-5 (exp. 5), which were synthesized, respectively, at 110 and 90°C in a medium of aliphatic hydrocarbons (undecane or heptane, respectively) in the presence of DBP. An increased temperature (110°C) produces a sharp drop in the content of Ti, OEt groups (Figure 1) and DBP (Table 2, compare exps 3 and 5). This may be related to a higher solubility of $\text{TiCl}_3(\text{OEt})$ complexes with DBP in a $\text{TiCl}_4/\text{C}_{11}$ medium at 110°C , which results in their removal from TMC-5.

Phase composition by X-ray data

Figure 2 shows XRD patterns (after subtraction of XRD pattern of the sample holder) for the studied catalysts and simulated XRD patterns for $\alpha\text{-MgCl}_2$ at different turbostratic disorder degrees (Figure 3). As it was shown earlier by the examples of graphite-like carbon [20] and aerogel Mg-V hydroxide [23], such XRD patterns are typical of turbostratically disordered materials. Such a disorder can arise in layered materials and appears as random shifts or rotations of layers.

XRD patterns of the studied samples indicate that, irrespective of the synthesis conditions, all the catalysts contain MgCl_2 : the (003) peak, a broad joint peak for two overlapping peaks (006) and (104)), and the (110) peak (Figure 2a). Assignment of the peaks is shown on Figure 3 (pattern 1) for the MgCl_2 crystallite consisting of six Cl-Mg-Cl layers and having a size of 6 nm. The shape of the second broad peak makes it possible to estimate approximately the turbostratic disorder degree in the MgCl_2 structure by comparing the experimental pattern with the simulated ones. XRD patterns of TMC-1 (Figure 2, pattern 1) and TMC-3 (pattern 3) are close to the simulated pattern 3 (Figure 3): they have the same shape of the second peak with the double apex. Table 3 lists data on crystallite sizes in directions [001] and [110] for the studied catalysts.

It is seen that in the TMC-2 catalyst (Figure 2, pattern 2) the MgCl_2 structure differs from that in TMC-1 or TMC-3. This is indicated by the shape of the broad second peak that looks like asymmetric triangle with a single apex. XRD pattern of this catalyst is similar to the simulated pattern 5 (Figure 3), which corresponds to MgCl_2 with a completely disordered structure (TDD ~ 1).

Two 2θ regions can be distinguished on the XRD pattern of the TMC-5 catalyst (Figure 2, pattern 4). The first region, $2\theta < 20^\circ$, is represented by a wide set of narrow peaks with different intensities, and the second region includes two broad peaks at $2\theta = 28\text{-}38^\circ$ and $2\theta = 50^\circ$, which belong to the MgCl_2 structure. A broad peak at $2\theta = 28\text{-}38^\circ$, which results from overlapping of two peaks, (006) and (104), has

asymmetric triangular shape and a single apex, as on the simulated XRD pattern with TDD ~ 1 (Figure 3, pattern 5). A set of narrow peaks at $2\theta = 20^\circ$ testifies that, in addition to MgCl_2 , there is also the second well crystallized phase, which is difficult to identify. Taking into account the high content of DBP and Ti in TMC-4 and the X-ray data reported in [22], which indicate that the crystal molecular complex $\text{TiCl}_4 \cdot \text{DEP}$ can appear in a TiCl_4 /hexane medium, one can suppose that a set of narrow peaks in the region of $2\theta < 20^\circ$ belongs to the crystal phase of molecular complexes $\text{TiCl}_3(\text{OEt}) \cdot m \text{DBP}$ and/or $\text{TiCl}_4 \cdot n \text{DBP}$. Thus, the TMC-4 catalyst consists most likely of two phases: MgCl_2 with a completely disordered structure and a well crystallized phase with non-identified composition, which may be represented by molecular complexes $\text{TiCl}_3(\text{OEt}) \cdot m \text{DBP}$ and/or $\text{TiCl}_4 \cdot n \text{DBP}$. Note that the average sizes of MgCl_2 crystallites for TMC-5 are close to those for TMC-2 (Table 3), which was synthesized without DBP and has also a high content of titanium and ethoxy groups. Evidently, the synthesis conditions of TMC-2 and TMC-5 do not ensure such a complete formation of MgCl_2 crystallites as in the case of TMC-1 and TMC-3 catalysts.

The TMC-1 and TMC-3 catalysts, which were synthesized in the presence of DBP at a titanation temperature of 110°C , have a less disordered structure and a greater size of MgCl_2 crystallites in direction [110] as compared to TMC-2 and TMC-5.

Thus, variation of the synthesis conditions of titanium-magnesium catalysts (the presence of DBP, features of the solvent, and temperature of titanation in an aliphatic solvent) exerts a pronounced effect on the crystal structure of the resulting catalysts.

Pore structure of TMCs

The initial $\text{Mg}(\text{OEt})_2$ has a low specific surface area ($5 \text{ m}^2/\text{g}$). As follows from the data reported in previous sections, the chlorination of $\text{Mg}(\text{OEt})_2$ with titanium tetrachloride produces either MgCl_2 alone (TMC-1 and TMC-3) or MgCl_2 and the X-ray amorphous complex of MgCl_2 with $\text{TiCl}_3(\text{OEt})$ (TMC-2) or two crystal phases: MgCl_2 and the phase with a probable composition $\text{TiCl}_3(\text{OEt}) \cdot m \text{DBP}$ and/or $\text{TiCl}_4 \cdot n \text{DBP}$ (TMC-5). Differences in the phase composition of the catalysts and in the degree of MgCl_2 structural disorder manifest themselves in characteristics of their pore structure.

Data on the pore structure of catalysts are summarized in Table 3 and Figure 4 (a, b, c). According to XRD and chemical analysis data, the pore structure of the TMC-1 catalyst is formed by MgCl_2 , which has a disordered structure, with TiCl_4 and DBP adsorbed on its surface. TMC-1 possesses a mesoporous structure (Figure 4a, b) with a narrow pore size distribution of 2.9 nm (Figure 4c). Specific surface area of the catalyst is $275 \text{ m}^2/\text{g}$, and total pore volume (V_{total}) is $0.18 \text{ cm}^3/\text{g}$. The cumulative pore volume ($0.18 \text{ cm}^3/\text{g}$), which is the sum of incremental pore volumes for the mesopore size region of 2-100 nm, corresponds to the total pore volume (Table 3).

The TMC-2 catalyst, which was synthesized under the same conditions as TMC-1 but without DBP, has a texture that differs from TMC-1 and is characterized by higher values of total pore volume ($0.28 \text{ cm}^3/\text{g}$) (Table 3). However, the cumulative volume of 2-100 nm pores is much smaller ($0.17 \text{ cm}^3/\text{g}$) than the total pore volume ($0.28 \text{ cm}^3/\text{g}$). This fact can indicate the presence of micropores with the diameter $<$

2 nm in TMC-2. A rough estimate made from the difference between total and cumulative pore volumes shows that the micropore volume (with the pore diameter < 2 nm) is 0.11 cm³/g. Thus, TMC-2 has the micro-mesoporous structure.

TMC-5 has low specific surface area (36 m²/g) and pore volume (0.055 cm³/g) (Table 3) at a broad pore size distribution (Figure 4 b, c). TMC-5 is a mixture of two phases: MgCl₂ with a completely disordered structure and the second well crystallized phase, which is expected to be TiCl₃(OEt)_mDBP and/or TiCl₄_nDBP. Each of the phases has its own textural characteristics, so the specific surface area and total pore volume are determined by the contribution of the surface area and pore volume of both phases. As was demonstrated for TMC-1, the presence of MgCl₂ alone and with a less disordered structure ensures high specific surface area and pore volume. This fact and the textural characteristics of TMC-5 allow a conclusion that the second crystallized phase constitutes a considerable fraction and makes the main contribution to the formation of the pore structure of TMC-5.

MgCl₂, which is formed under the synthesis conditions of TMC-3, has the same disordered structure and average size of crystallites as TMC-1. The specific surface area (194 m²/g) of TMC-3 is lower than that of TMC-1. Total pore volume (0.16 cm³/g) of TMC-5 is comparable with the pore volume of TMC-1, but TMC-3 has a broader pore volume distribution and inhomogeneous porosity: there are mesopores with the size of 2.9 nm, which are typical and prevailing in TMC-1, and pores with the size of 4-80 nm, which are typical of the pore structure of TMC-5 (Figure 4c).

Activity and stereospecificity of TMCs in polymerization of propylene

Data on the catalyst activity and stereospecificity (the APP content) in polymerization of propylene are listed in Tables 2 and 3. Of all the catalysts, the highest activity and stereospecificity were observed for TMC-1 (exp. 1). Activity and stereospecificity of TMC-4 (exp. 4) are close to those of the TMC-1 catalyst.

Activity of TMC-2 is much lower in comparison with TMC-1, especially as referred to gram of titanium. A high content of APP testifies to a low stereospecificity of the catalyst. The low activity and stereospecificity of TMC-2 are caused by the high content of OEt groups and the absence of a stereoregulating donor (DBP).

Data on the influence of OEt groups content on activity and stereospecificity of TMCs in propylene polymerization were previously reported in [3, 8] with respect to catalysts Mg(OEt)₂/benzoyl chloride/TiCl₄. It was shown that increasing the number of treatments of solid intermediate products with TiCl₄ or TiCl₄/ChB resulted in decreasing of OEt groups content from a few percent to fraction of a percent. In this case, there was an increase in the activity and stereospecificity of catalysts which was due to the removal of OEt groups from the catalyst. According to our data, OEt groups are part of the by-product TiCl₃(OEt), which is inactive in propylene polymerization [24].

TMC-5 (exp. 5) has the lowest activity (0.6 kg PP/(g_{cat}·h)) and low stereospecificity (APP = 13.4 wt.%). The low activity and stereospecificity of TMC-5, which was synthesized in a TiCl₄/C₇ medium at 90°C and in the presence of DBP, may be caused by several factors, which distinguish it from the highly

active catalyst TMC-1: i) a high titanium content (6.7 wt.%) at virtually the same distribution of titanium as TiCl_4 and $\text{TiCl}_3(\text{OEt})$ ($\text{OEt}/\text{Ti} = 0.44$); ii) the involvement of DBP in the formation of the $\text{TiCl}_3(\text{OEt})\cdot m\text{DBP}$ complex and/or $\text{TiCl}_4\cdot n\text{DBP}$ as an individual phase, which is inactive in the polymerization process; iv) the pore structure of the catalyst (very low specific surface area and total pore volume, and a broad pore size distribution).

Note that stereospecificity of TMC-5, which was synthesized with DBP, is as low as that of the phthalate-free catalyst TMC-2. This fact indicates that DBP, which is present in the composition of TMC-5, does not serve as the internal stereoregulating donor.

Activity of TMC-3 is two times lower as compared to that of TMC-1. This may be related to a lower specific surface area of the catalyst and a broader pore size distribution. The decreased activity and stereospecificity of TMC-3 may be caused also by the inhibiting action of phthaloyl chloride, which is formed in a large amount (5 wt. %) upon synthesis of this catalyst and, according to data reported in [21], deteriorates the activity and stereospecificity of TMCs.

CONCLUSION

Supported catalysts were synthesized via the interaction of $\text{Mg}(\text{OEt})_2$ with TiCl_4 in the presence or absence of an internal stereoregulating donor (DBP), with different solvents (chlorobenzene, heptane, undecane) and at different titanation temperatures (110 and 90°C). Data on the chemical composition of these catalysts, the crystal structure of MgCl_2 formed during the catalyst synthesis, the pore structure of the catalysts as well as their activity and stereospecificity in polymerization of propylene have been obtained.

The optimal catalyst TMC-1, which was synthesized in the presence of DBP in a chlorobenzene medium at 110°C, has high activity and stereospecificity. This catalyst contains the minimal amount of $\text{TiCl}_3(\text{OEt})$ by-product, has a more ordered X-ray structure and a homogeneous mesoporous structure with a narrow pore size distribution.

Elimination of DBP from the catalyst synthesis (TMC-2) produces sharp changes in the chemical composition, crystal and pore structure, and substantially decreases activity and stereospecificity. The content of titanium and ethoxy groups in the catalyst sharply increases because a great part of titanium is present in the catalyst as $\text{TiCl}_3(\text{OEt})$. MgCl_2 , which is formed under the synthesis conditions of this catalyst, has a maximum disorder of the crystal structure and a lesser size of crystallites. The catalyst has a micro-mesoporous structure with a significant contribution from micropores (< 2 nm) to total pore volume. According to the comparative data obtained for the catalysts TMC-1 and TMC-2, a stereoregulating donor (DBP) is directly involved in the formation of final catalyst via removal of $\text{TiCl}_3(\text{OEt})$ by-product and formation of MgCl_2 with optimal crystalline and pore structures.

The replacement of chlorobenzene by non-aromatic hydrocarbon *n*-undecane as a solvent in the synthesis of catalyst at 110°C in the presence of DBP (TMC-3) results in the formation of a catalyst whose chemical composition and structural characteristics of MgCl_2 are close to the catalyst synthesized with chlorobenzene (TMC-1). However, this catalyst has a high content of phthaloyl chloride, a lower

specific surface area and a broad pore size distribution. These factors determine a lower activity of this catalyst in comparison with TMC-1, which was synthesized with chlorobenzene. A decrease in the synthesis temperature to 90°C (TMC-5) instead of 110°C with the use of non-aromatic solvent (*n*-heptane) leads to crucial changes in the chemical composition, structure and performance of the catalyst in propylene polymerization. The high content of titanium, ethoxy groups and DBP is related with inhomogeneous phase composition of the catalyst, namely, with the presence of not only MgCl₂ having a maximum structural disorder but also of the second phase with a well crystallized structure, which is represented most likely by molecular complexes TiCl₃(OEt)·*m*DBP and/or TiCl₄·*n*DBP that are stable under the synthesis conditions. A very low specific surface area and low total volume of pores are caused by the high content of this phase and its prevailing contribution to the formation of the catalyst pore structure. This catalyst has the lowest activity and stereospecificity among all the catalysts studied in the work. Stereospecificity of TMC-5 is low because in this catalyst DBP is present mostly as a by-product, the TiCl₃(OEt)·DBP complex (and/or TiCl₄·DBP), and does not serve as the stereoregulating internal donor.

Thus, the chemical composition, structure, activity and stereospecificity of the catalysts synthesized via the interaction of Mg(OEt)₂ with TiCl₄ depend on the presence of a stereoregulating electron donor component, the nature of solvent and titanation temperature. Therewith, activity and stereospecificity of the catalysts are determined by the following characteristics:

- 1) The chemical composition, in particular, the presence of inactive by-products formed during the interaction of Mg(OEt)₂ with TiCl₄ in case of TMC-2 and TMC-5 catalysts: (TiCl₃(OEt) and complexes TiCl₃(OEt)·*m*DBP or TiCl₄·*n*DBP).
- 2) The structure of MgCl₂: low active catalysts TMC-2 and TMC-5 have a completely disordered structure of MgCl₂ and a small size of crystallites. Highly active catalysts TMC-1 and TMC-3 have a more ordered crystal structure and a greater size of crystallites.
- 3) The pore structure: the most active catalyst TMC-1, in distinction to all other catalysts, has a homogeneous mesoporous structure and a narrow pore size distribution.

ACKNOWLEDGEMENTS

The authors thank Dr. Bukatov G.D. (Boreskov Institute of Catalysis SB RAS) for valuable discussions of the obtained results. This work was supported by Russian Academy of Sciences and Federal Agency of Scientific Organizations (project V.44.2.1).

REFERENCES

1. Shijng X, Honglan L, Inghui Z (1990) Studies on $\text{TiCl}_4/\text{Mg}(\text{OEt})_2/\text{EB}$ supported catalysts catalyst for propylene polymerization. *Chinese J Polym Sci* 8: 253-260
2. Jeong Y-T, Lee D-H (1990) Propene polymerization with $\text{Mg}(\text{OEt})_2$ supported TiCl_4 catalyst, 1. Catalyst composition and behavior. *Macromol Chem* 191: 1487-1496
3. Jeong Y-T, Lee D-H, Soga K (1991) Propene polymerization with $\text{Mg}(\text{OEt})_2$ -supported TiCl_4 catalyst, 2^a). Effects of TiCl_4 treatment. *Macromol Chem, Rapid Commun* 12: 5-7
4. Jeong Y-T, Lee D-H, Shiono T, Soga K (1991) Propene polymerization with $\text{Mg}(\text{OEt})_2$ -supported TiCl_4 catalyst. 3^a) The role of benzoyl chloride. *Macromol Chem* 192: 1727-1731
5. Lee D-H, Jeong Y-T, Soga K, Shiono T (1993) Propene polymerization with $\text{Mg}(\text{OEt})_2/\text{benzoyl chloride}/\text{TiCl}_4$ -triethylaluminum/external donor catalyst systems. *J Appl Polym Sci* 47: 1449-1461
6. Lee D-H, Jeong Y-T (1993) Propene polymerization with $\text{Mg}(\text{OEt})_2$ -supported TiCl_4 catalyst. – 4. Effect of hydrogen. *Eur Polym J* 29: 883-888
7. Chadwick JC, Miedema A, Ruish BJ, Sudmeijer O (1992) Effects of procatalyst composition on the stereospecificity of a Ziegler-Natta catalyst system. *Makromol. Chem* 193: 1463-1468
8. Kim I, Choi HK, Han TK, Woo SI (1992) Polymerization of propylene catalyzed over highly active and stereospecific catalysts synthesized with $\text{Mg}(\text{OEt})_2/\text{Benzoyl Chloride}/\text{TiCl}_4$. *J Polym. Sci, Part A: Polym Chem* 30: 2263-2271
9. Lee D-H, Jeong Y-T, Kang KK (1994) Change of internal donor for $\text{Mg}(\text{OEt})_2$ –supported TiCl_4 catalysts. *Catalyst design for tailor-made polyolefins* 89: 153-163
10. Kang KK, Shiono T, Jeong Y-T, Lee D-H (1999) Polymerization of propylene by using $\text{Mg}(\text{OEt})_2$ –DNBP- TiCl_4 Catalyst with disilanes as external Donor. *J Appl Polym Sci* 71: 293-301
11. Kang KK, Kim K, Lee D-H, Jeong Y-T (2001) Propene polymerization by using TiCl_4 catalyst supported on solvent activated $\text{Mg}(\text{OEt})_2$. *J Appl Polym Sci* 81: 460-467
12. Tanase S, Katayama K, Inasawa S, Okada F, Yamaguchi Y, Sadashima T, Yabunouchi N, Konakazawa T, Junke T, Ishihara N (2008) New synthesis method using magnesium alkoxides as carrier materials for Ziegler-Natta catalysts with spherical morphology. *Macromol React Eng* 2: 233-239
13. Tanase S, Katayama K, Inasawa S, Okada F, Yamaguchi Y, Konakazawa T, Junke T, Ishihara N (2008) Particle growth of magnesium alkoxide as carrier material for polypropylene polymerization catalyst. *Appl Catal A: Gen* 350: 197-206

14. Dashti A, Ahmad Ramazani SA, Hiraoko Y, Kim SY, Tanlike T, Terano M (2009) Kinetic and morphological study of a magnesium ethoxide-based Ziegler-Natta catalyst for polypropylene polymerization. *Polym International* 58: 40-45
15. Taniike T, Funako T, Terano M (2014) Multilateral characterization for industrial Ziegler-Natta catalysts toward elucidation of structure-performance relationship. *J Catal* 311: 33-40
16. Funako T, Chammingkwan P, Taniike T, Terano M (2015) Alternation of pore architecture of Ziegler-Natta catalysts through modification of magnesium ethoxide. *Macromol React Eng* 9: 325-332
17. Makwana UC, Singala KJ, Patankar RB, Singh SC, Gupta VK (2012) Propylene polymerization using supported Ziegler-Natta catalysts systems with mixed donors. *J Appl Polym Sci* 125: 896-901
18. Chumachenko NN, Zakharov VA, Bukatov GD, Sergeev SA (2014) A study of the formation process of titanium-magnesium catalyst for propylene polymerization. *Appl Catal A-Gen* 469: 512-516
19. Cherepanova SV, Tsybulya SV (2000) Simulation of X-ray powder diffraction patterns for low-ordered materials. *J Mol Catal A-Chem* 158: 263-266
20. Cherepanova SV, Tsybulya SV (2004) Simulation of X-ray powder diffraction patterns for one-dimensionally disordered crystals. *Mater Sci Forum* 443-4: 87-90
21. Arzoumanidis GG, Karayannis NM (1991) Infrared spectral characterization of supported propene polymerization catalysts. A link to catalyst performance. *Appl Catal* 76: 221-231
22. Utko J, Sobota P, Lis T (1987) The crystal structure of tetrachloro(diethylphthalate)titanium (IV). *J Organomet Chem* 334: 341-345
23. Ilyina EV, Mishakov IV, Vedyagin AA, Cherepanova SV, Nadeev AN, Bedilo AF, Klabunde KJ (2012) Synthesis and characterization of mesoporous V_{Ox}/MgO aerogels with high surface area. *Micropor Mesopor Mater* 160: 32-40
24. Garoff T, Iiskola E, P. Sormunen P (1988) The influence of crystal water on the performance of Ziegler-Natta catalyst in propylene polymerization. In: Kaminsky WH, Sinn H (Eds.), *Transition metals and organometallics as catalysts for olefin polymerization*. Springer-Verlag, Berlin-Heidelberg, 197-208

Symbols and Abbreviations

ACS – average crystallite size

Al(Et)₃ - triethylaluminum

APP – atactic polypropylene

ChB – chlorobenzene

D – average pore diameter

DBP – di-*n*-butyl phthalate

DEP – diethyl phthalate

EBP – ethyl butyl phthalate

PC – phthaloyl dichloride (1, 2-benzenedicarbonyl dichloride)

PP – polypropylene

PrSi(OMe)₃ – propyltrimethoxysilane

S_{BET} – specific surface area

TDD – turbostratic disorder degree

V_{total} – total pore volume

V_i – incremental pore volume

V_i^{max} – maximum incremental pore volume

XRD – X-ray diffraction method

Accepted Manuscript (POJ)

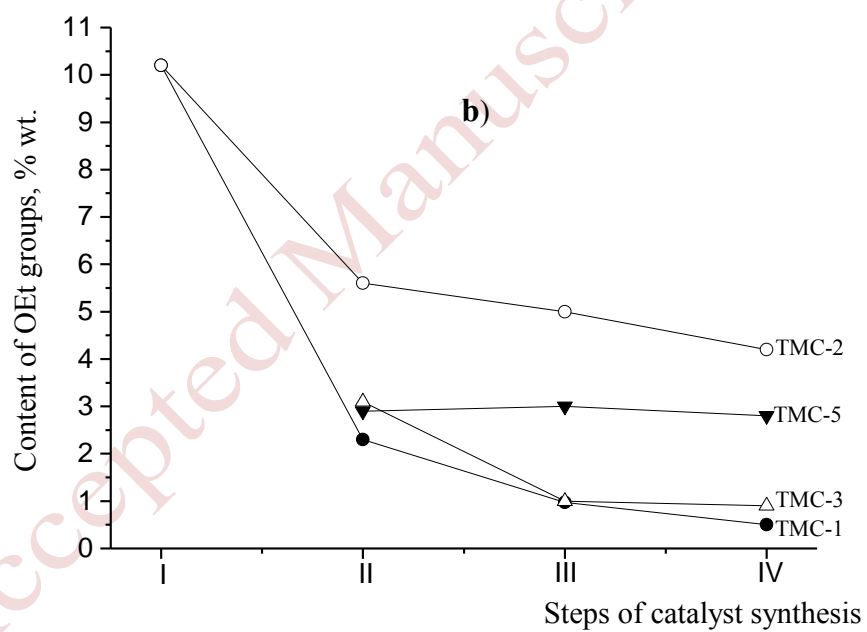
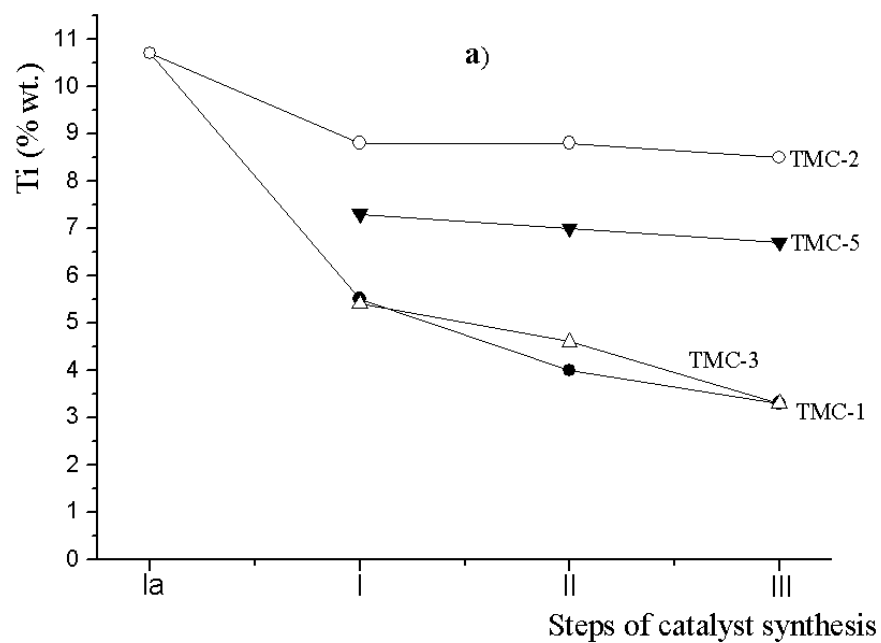


Figure 1. Content of Ti (a) and OEt-groups (b) in solid products formed during TMC synthesis.

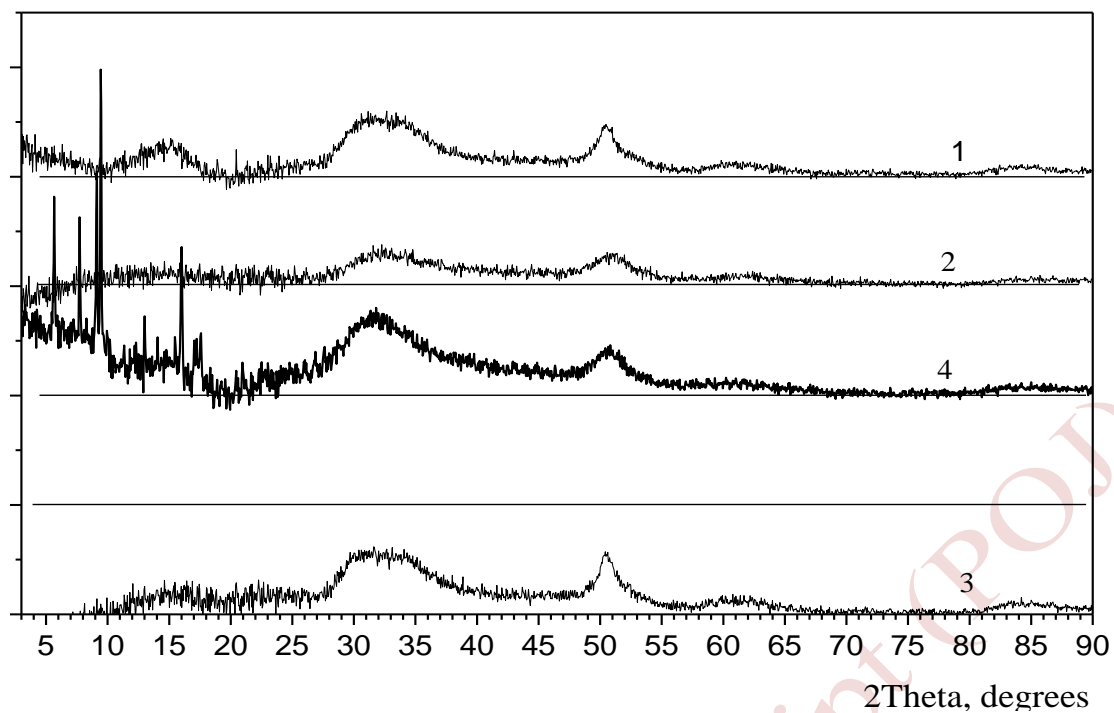


Figure 2. Experimental XRD patterns of catalysts from Table 3: TMC-1 (1), TMC-2 (2), TMC-3 (3), TMC-5 (4).

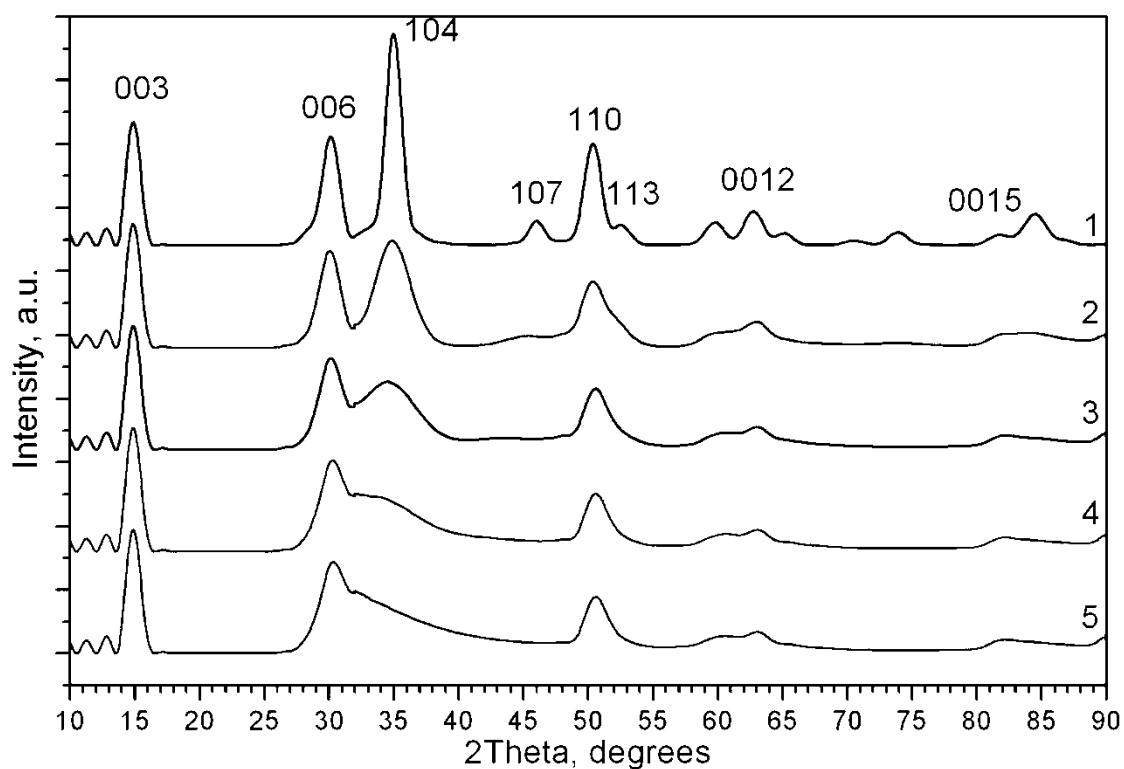


Figure 3. XRD patterns simulated for MgCl_2 with the same average crystallite size of 6 nm and different TDDs equal to 0 (1), 0.2 (2), 0.4 (3), 0.6 (4), 1.0 (5).

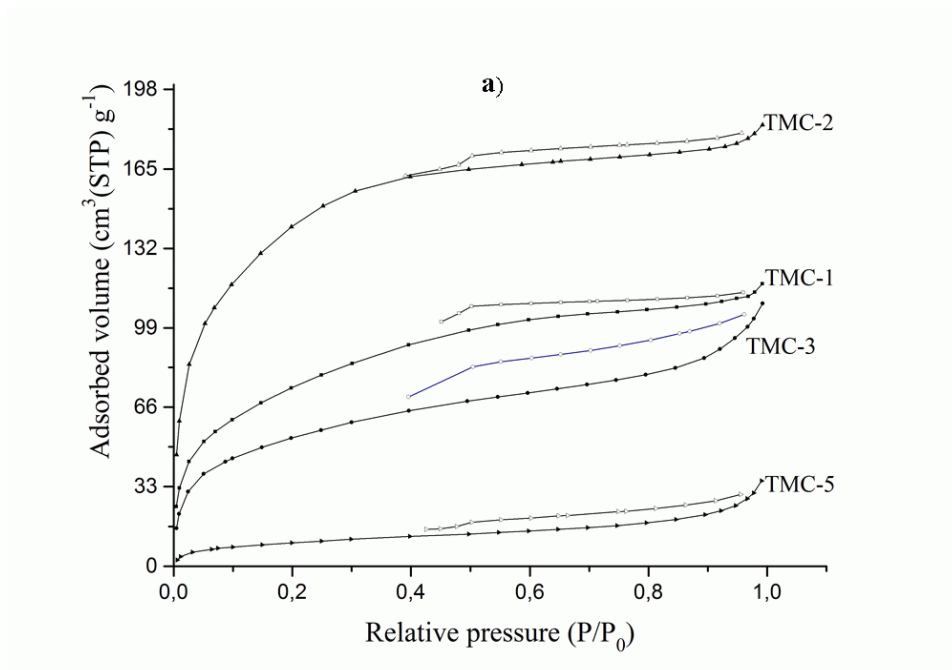


Figure 4a. N₂ adsorption /desorption isotherms for examined catalysts.

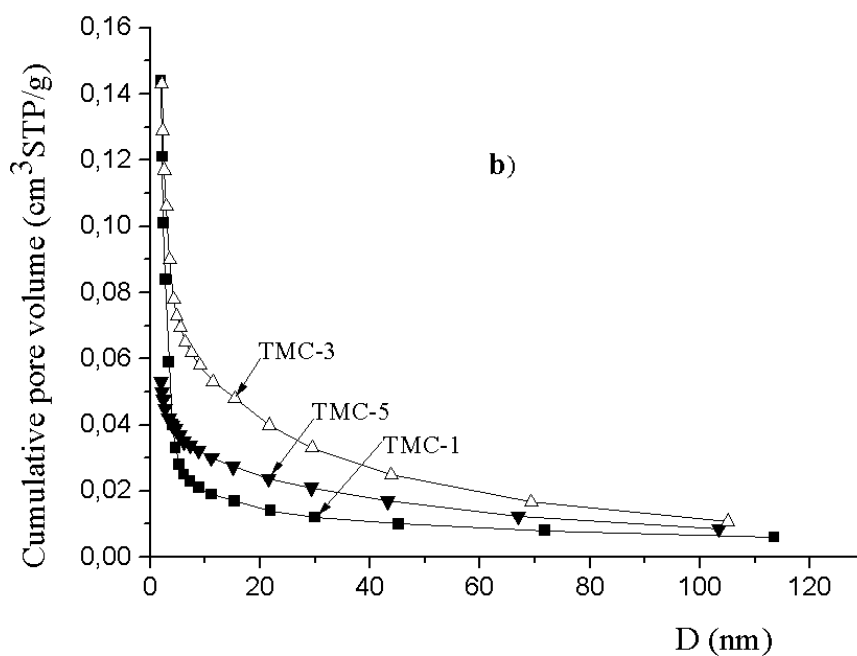


Figure 4b. Cumulative pore volume distribution vs. average pore diameter.

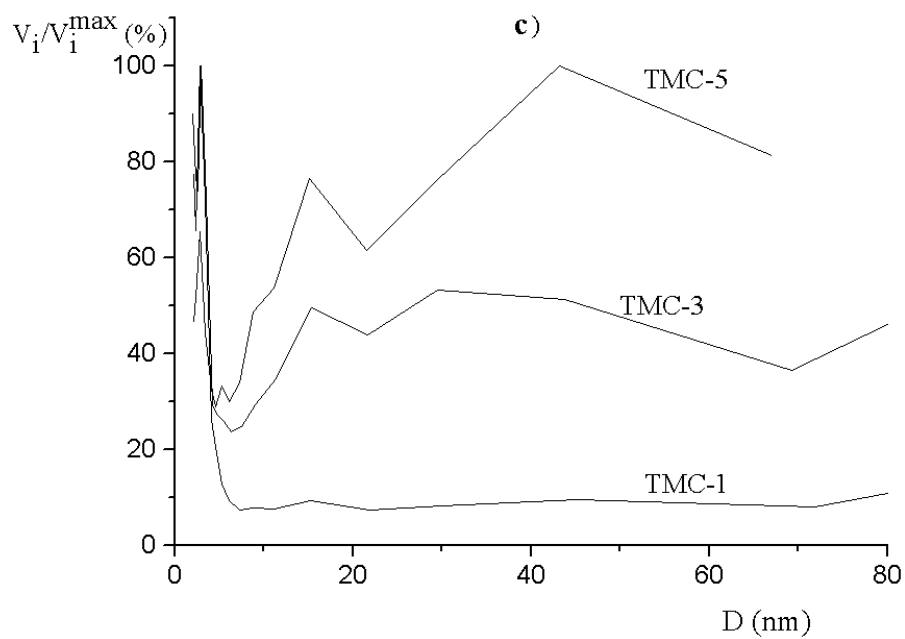


Figure 4c. Incremental pore volume distribution (V_i) as a percentage of the maximum incremental pore volume (V_i^{\max}) vs. average pore diameter.

Table 1. General parameters of TMC-PP preparation.

Catalyst	TMC-PP preparation		
	Internal donor (DBP)	Solvent	Temperature (°C)
TMC-1	+	chlorobenzene	110
TMC-2	-	chlorobenzene	110
TMC-3	+	<i>n</i> -undekane	110
TMC-4	+	chlorobenzene	90
TMC-5	+	<i>n</i> -heptane	90

Table 2. Data on chemical composition and polymerization results for TMC-PP catalysts.

Exp. No.	Catalyst	Content (wt. %)					Molar ratio (mol/mol)				(kg PP/ (g _{Ti} · h))
		Ti	Mg	Cl	OEt	DBP	$\frac{\text{Ti}}{\text{Mg}}$	$\frac{\text{DBP}}{\text{Mg}}$	$\frac{\text{DBP}}{\text{Ti}}$	$\frac{\text{OEt}}{\text{Ti}}$	
1	TMC-1	3.3	18.8	62.0	0.5	11.5 ¹⁾	0.09	0.053	0.60	0.16	
2	TMC-2	8.5	16.7	65.6	4.2	-	0.26	-	-	0.53	
3	TMC-3	3.3	18.6	57.0	0.9	11.3 ²⁾	0.09	0.053	0.59	0.29	
4	TMC-4	3.4	18.0	60.0	0.5	9.4	0.096	0.046	0.048	0.16	
5	TMC-5	6.7	14.0	51.6	2.8	19.3	0.24	0.12	0.50	0.44	

¹⁾ Along with DBP the catalyst TMC-1 contains 1 wt. % of (EBP + DEP).

²⁾ The catalyst TMC-3 contains complementary 0.55 wt. % of (EBP + DEP) and 5 wt. % of phthaloyl dichloride.

Table 3. Structural data and activity for TMC-PP-catalysts.

Catalyst	X-ray data			Porous structure				Activity	
	Interplaner distances (nm)	ACS ¹⁾ in [001] direction (normal to layers) (nm)	ACS ¹⁾ in [110] direction (along layers) (nm)	S _{BET} (m ² /g)	V _{total} (cm ³ /g)	V ₁ ²⁾ (cm ³ /g)	V ₂ ³⁾ (cm ³ /g)	(kg PP/ (g _{CAT} · h))	(kg PP/ (g _{Ti} · h))
TMC-1	0.59	2.0	6.4	275	0.18	0.18	0	10.4	315
TMC-2	0.61	1.4	3.6	-	0.28	0.17	0.11	3.9	45.9
TMC-3	0.61	1.9	7.6	194	0.17	0.14	0	5.0	152
TMC-5	0.61	1.9	4.3	36	0.055	0.050	0	0.6	9.0

¹⁾ Average crystallite size

²⁾ V₁ – cumulative pore volume (pore diameter 2-100 nm)

³⁾ V₂ – micropore volume (pore diameter < 2 nm).